STUDIES ON THE IONIC PERMEABILITY OF MUSCLE CELLS AND THEIR MODELS

GILBERT N. LING *and* MARGARET M. OCHSENFELD

From the Department of Molecular Biology in the Department of Neurology, Division of Medicine, Pennsylvania Hospital, Philadelphia

ABSTRACT We studied the effect an alkali-metal ion exercised on the rate of entry of another alkali-metal ion into frog sartorius muscle cells and their models (*i.e.*, ion exchange resin and sheep's wool). In the case of frog muscle, it was shown that the interaction fell into one of four categories; competition, facilitation, and two types of indifference. The observed pK value (4.6 to 4.7) of the surface anionic groups that combine with the alkali-metal ions suggests that they are β- or γ-carboxyl groups of proteins on the cell surface. The results were compared with four theoretical models which included three membrane models (continuous lipoid membrane with carrier; leaky membrane with carrier; membrane with fixed ionic sites) and one bulk-phase model. This comparison led to the conclusion that the only model that is self-consistent and agrees with all of the experimental facts is the one based on the concept that the entire living cell represents a proteinaceous fixed-charge system; this model correctly predicts all four types of interaction observed.

INTRODUCTION

Before the turn of the 20th century, Overton studied the rates of penetration of dyes into animal and plant cells and compared the data with the lipid solubilities of these dyes. From the correlation he discovered, he suggested that a continuous membrane of lipid material surrounds the cell (1). Glucose, amino acids, and electrolytes; all of which are lipoid-insoluble, do, nevertheless, enter the cells. Overton interpreted this fact as being due to some sort of secretive process ("adenoid" activity). Later, studying the diffusion of ammonia (NH_3) into *Valonia* cells, Osterhout (2), see also Jacques (3), postulated that the bulk of the cell membrane is also impermeable to NH_3. However, NH_3 could enter the cell by first combining with an acid constituent of the cell membrane at its outer surface; this NH_3 complex then would traverse the bulk of the cell membrane and discharge the NH_3 into the intracellular water at the inner surface. Subsequently, observations similar to Osterhout's were made on ionic permeability into barley roots (4), frog muscle cells (5, 6), yeast cells (7), and Ehrlich ascites cells (6). In all these cases,

the rate of entry does not increase linearly with increasing concentration of ion in the external medium but shows "saturability;" *i.e.*, the rate of entry approaches a constant value as the external ionic concentration approaches infinity. Quantitative analyses of these entry data have often been made on the basis of a mathematical formulation similar to that of Michaelis and Menten for enzyme kinetics (see below). The majority of investigators have invoked a carrier hypothesis to interpret the saturability phenomena observed experimentally. In a 1954 review, Danielli classified such carrier-mediated permeation into two categories. (*a*) "Active transport" refers to a postulated pump-like mechanism by means of which a solute is moved against a concentration gradient; active transport is thus considered instrumental in maintaining the steady-state concentration gradient of solutes between the intra- and extracellular phases, a well known example is the postulated Na pump. (*b*) "Facilitated diffusion" refers to another type of carrier-mediated permeation in which the solute does not move up-hill against a concentration gradient. A third type of permeation, according to Danielli, does not show saturability and is refered to simply as "diffusion" (8).

Experimental studies first reported in 1953 (5, 6) led Ling to present an alternative thesis whereby ionic permeation that shows saturability is attributed to the association of the entrant ion with fixed ionic sites of the opposite sign on and near the cell surface and subsequent dissociation from these sites. This thesis, which is part of a general theory called the association-induction hypothesis (first known as the fixed-charge hypothesis), is based on evidence that the entire living cell constitutes a fixed-charge system.[1] In this system the cell proteins form a three dimensional matrix which polarizes and orients the water molecules in multilayers. Since such polarized water partially excludes solutes (14), a solute tends to exist at a lower concentration in the cell water than in the external medium. If, however, the solute associates with ionic or hydrogen-bonding sites in the cell, the intracellular concentration of the solute may reach a concentration many times higher than that in the external medium (15). Differences in the free energy of association of various solutes then provide the basis for selectivity both in solute permeation (due to surface sites) and in solute accumulation (due to sites in the bulk phase protoplasm). According to this view, selective ionic permeability is a partial expression of the phenomenon of selective ionic accumulation and not its cause (unlike various versions of the membrane theory); nor is there a need to divide permeation that shows saturability into passive "facilitated" diffusion and active transport.

---

[1] Since several recent reviewers have not been clear on this issue, it bears pointing out that there are fixed ionic sites on the cell membrane as was recognized by Michaelis (9), Teorell (10), and Sollner (11) long ago. The postulation that association of ions and other solutes with fixed sites is the basic mechanism in selective accumulation (12, 13) and selective permeability (15) in living cells was, on the other hand, introduced as part of what is now known as the association-induction hypothesis.

Abstracts and a review (but no detailed description) of the present work have appeared on different occasions (5, 6). In this communication, following a review of the theoretical concepts that are sufficiently developed to allow quantitative analysis, we will present new experimental work in detail and discuss it in the light of the alternative models.

THEORY

We shall examine the qualitative aspects of several theoretical models with particular emphasis on the effect of the presence of one ion in the external medium on the rate of inward permeation of another. These models include three membrane models and a bulk-phase model.

Model I: Impermeable membrane-carrier model, Overton (1) and Osterhout, (2).

In this model a continuous lipoid membrane is postulated to surround the cell and is assumed to be absolutely impermeable to ions. The only way for an ion to enter or leave the cell is by complexing with a "carrier" in the lipoid membrane. For such a system Epstein and Hagen (4) have written

$$R + M_{\text{outside}} \underset{k_2}{\overset{k_1}{\leftrightarrows}} MR, \tag{1}$$

and

$$MR \underset{k_4}{\overset{k_3}{\leftrightarrows}} R' + M_{\text{inside}}, \tag{2}$$

where R and R' represent different chemical states of the metabolically produced carrier. M is the ion, MR is the metastable carrier-ion complex, and k, the rate constant for each reaction indicated. On the basis of the above reaction, they were able to apply the Michaelis-Menten formulation of enzyme kinetics to ion transport:

$$V_i = \frac{V_i^{\max}[p_i]_{ex}\tilde{K}_i}{1 + [p_i]_{ex}\tilde{K}_i + [p_j]_{ex}\tilde{K}_j}, \tag{3}$$

where $\tilde{K}_i$ and $\tilde{K}_j$ are the association constants of the ith ion and jth ion with the carrier respectively. V_i and $V_i^{\max}$ are the observed and maximum rate of ion entry respectively. $[p_i]_{ex}$ and $[p_j]_{ex}$ are the concentrations of the entrant ion, i, and the inhibiting ion, j, in the external medium. Equation 3 predicts that, for each fixed concentration of the competing ion, $[p_j]_{ex}$, a plot of $1/[p_i]_{ex}$ against $1/V_i$ yields a straight line; a family of such lines for different values of $[p_j]_{ex}$ joins at the same locus on the ordinate. A similar formulation has been given by Wilbrandt and Widdas and their associates for the permeation of sugars into cells (16, 17).

Model II: Leaky membrane-carrier model.

If the membrane is not absolutely impermeable to ions or if there are aqueous

channels in the cell membrane, the initial rate of inward migration may be expressed[2] as:

$$V_i = A[p_i]_{ex} + \frac{V_i^{max}[p_i]_{ex}\tilde{K}_i}{1 + [p_i]_{ex}\tilde{K}_i + [p_j]_{ex}\tilde{K}_j}. \quad (4)$$

In this equation the first term refers to diffusion through the aqueous channels (or leakage); the second term refers to carrier-mediated transport. A, the specific rate of inward leakage, is a constant. V_i^{max} is the maximum rate of entry of the ith ion *via* the carrier.

Model III: Bulk phase model; the entire cell as a proteinaceous fixed-charge system.

Fig. 1 shows a microscopic portion of the surface of a fixed-charge system; the two types of ionic entry from the external solution, the *saltatory route* and the *adsorption-desorption route* are depicted (see reference 6, section 11.2A). The saltatory route resembles a free diffusion process, it is independent of the fixed ions and their adsorbed counterions and thus has the behavior of a first order reaction. The adsorption-desorption route, on the other hand, represents a heterogenous process and may be divided further into triplet or doublet adsorption-desorption depending on whether or not the entrant ion leaves the fixed ionic site with the aid of a second free ion. Theoretically it is possible to expose the cell to the ion under study so briefly, that entry involves adsorption only on the very first layer of fixed

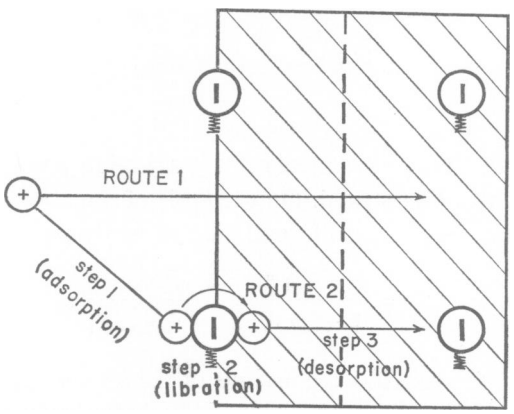

FIGURE 1 *Diagrammatic illustrations of the two routes of ion entry into a fixed-charge system.* Shaded area represents a microscopic portion of the surface of a fixed-charge system in which four fixed anions are represented. Route 1 is the saltatory route. Route 2, the adsorption-desorption route, involves a sequence of three steps; adsorption, libration around the fixed anion, and desorption. This adsorption-desorption route corresponds to the doublet type, since two ions are involved (the free cation and the fixed anion). See Fig. 24 for another variety.

[2] This model, of course, implies two-way leakage (both inward and outward) and is not to be confused with some other models recently proposed assuming one-way leakage. Such an assumption violates the second law of thermodynamics.

anionic sites. In this case, the total rate of inward entry of an ion is the sum of the rates of entry *via* the three routes. For comparison with the other models, the explicit equation (equation 15 in the Appendix) may be written as follows:

$$V = A[p_i]_{ex} + \frac{V_i^{max}\tilde{K}_i[p_i]_{ex}}{1 + \tilde{K}_i[p_i]_{ex} + \tilde{K}_j[p_j]_{ex}} + \frac{V_{ii}^{max}\tilde{K}_i\tilde{K}_{ii}[p_i]^2}{\{1 + \tilde{K}_i[p_i]_{ex} + \tilde{K}_j[p_j]_{ex}\}\{1 + \tilde{K}_{ii}[p_i]_{ex} + \tilde{K}_{ij}[p_j]_{ex}\}} + \frac{V_{ij}^{max}\tilde{K}_i\tilde{K}_{ij}[p_i][p_j]}{\{1 + \tilde{K}_i[p_i]_{ex} + \tilde{K}_j[p_j]_{ex}\}\{1 + \tilde{K}_{ii}[p_i]_{ex} + \tilde{K}_{ij}[p_j]_{ex}\}}. \quad (5)$$

The first term of this equation describes the saltatory route; the second, the doublet route. The third and fourth terms describe two types of entry *via* the triplet adsorption-desorption route. If we represent a fixed ion as *f*, a second ion or molecule of the same species (*i.e.*, the *i*th) may activate the dissociation of the fixed ion-*i*th ion pair ($i \rightarrow f.i$) causing the first *i*th ion to dissociate and enter the cell, or an ion of a different species, *j*, may activate *i*th ion entry ($j \rightarrow f.i$). In equation 5, V_{ii}^{max} and V_{ij}^{max} are the maximum rates of entry through these last two routes, respectively; $\tilde{K}_{ii}$ and $\tilde{K}_{ij}$ are the *i.f.i.* and *j.f.j.* triplet association constants respectively. The remaining symbols have the same meaning as in equation 4.

In Figs. 2 through 5, the reciprocals of the rates of *i*th-ion entry into living cells and other fixed-charge systems, calculated on the basis of equation 5 in its explicit form (equation 15), are plotted against the reciprocals of the *i*th-ion concentration. $[p_i^+]_{ex}$ refers to the concentrations of the *j*th cation also present in the system. The choice of the numerical values used in the calculations is explained in the Appendix.

Type 1: Competition. Fig. 2 depicts a case where doublet entry predominates.

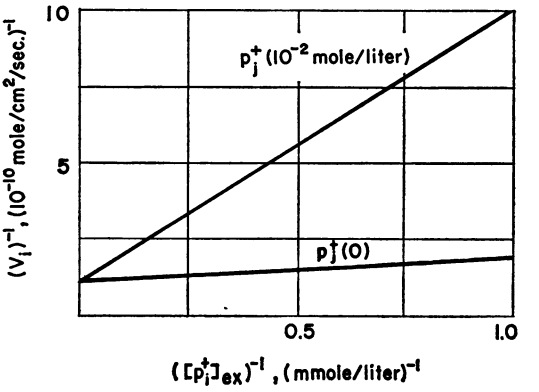

FIGURE 2 *Competition: Theoretical effect of p_j^+ on the rate of entry of p_i^+ (V_i), into fixed-charge system.* Reciprocal plot of theoretical values calculated from equation 15 (see Appendix). Numerical values used are $A = 10^{-10}$ (mole/second), $B = 10^{-7}$ (mole/second), $K_i^{ex} = K_j^{ex} = 10^3$ (mole/liter)$^{-1}$, exp $(-\Delta F_{if}^{\ddagger}/RT) = 10^{-3}$, exp $(-\Delta F_{jf}^{\ddagger}/RT) =$ exp $(\Delta F_{ijf}^{\ddagger}/RT) = 10^{-2}$; $C = D = 1$, $K_{ii}^{ex \cdot ex} = K_{ij}^{ex \cdot ex} = 1$ (mole/liter)$^{-1}$.

The reciprocal rate of entry, $1/V_i$, is plotted against the reciprocal of the *i*th-cation concentration $1/[p_i^+]_{ex}$, yielding a straight line for each concentration of *j*th competing ion. The family of lines produced by varying the concentrations of the *j*th ion converges toward one locus on the ordinate. The common intercept and the slopes of the lines can be used to determine the apparent association constants of the *i*th and *j*th ions.

Type 2: Facilitation. Fig. 3 depicts a case in which the *j*th cation has a predominantly facilitory action on the entry of the *i*th cation. The reciprocal plots

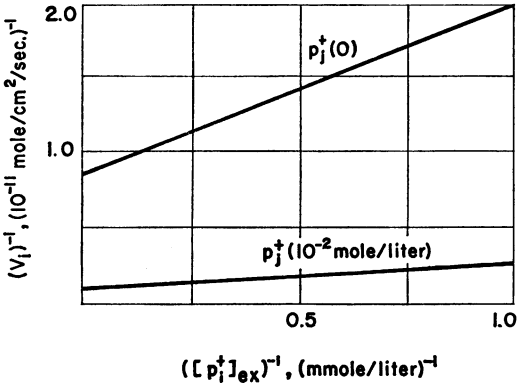

FIGURE 3 *Facilitation: Theoretical effects of p_j^+ on the rate of entry of p_i^+, (V_i), into a fixed-charge system.* Reciprocal plot of values calculated from equation 15. Numerical values used were: $A = 10^{-10}$ (mole/second), $B = 10^{-7}$ (mole/second), $K_i^{ex} = 10^3$ (mole/liter)$^{-1}$, $K_j^{ex} = 10^2$ (mole/liter)$^{-1}$, exp $(-\Delta F_{if}^{\ddagger}/RT) = 10^{-4}$, exp $(-\Delta F_{ifi}^{\ddagger}/RT) = 10^{-8}$, exp $\cdot(-\Delta F_{iff}^{\ddagger}/RT) = 10^{-1}$, $C = D = 1$, $K_{ii}^{ex \cdot ex} = K_{ij}^{ex \cdot ex} = 1$ (mole/liter)$^{-1}$.

in this case also yield straight lines, but these lines do not meet each other on the ordinates and the rate of entry increases as $[p_i^+]$ increases.

Type 3: Indifference. ($\tilde{K}_i \gg \tilde{K}_j$). Fig. 4 shows a case where the *i*th-cation entry is indifferent to the increase of the *j*th-cation concentration, because the association constant of the *i*th-cation ($\tilde{K}_i$) is much larger than that of the *j*th-ion (*i.e.*, $\tilde{K}_i \gg \tilde{K}_j$). Since the *i*th-cation association energy is high, there is distinct competition among the *i*th-cations themselves. Thus, if the entry of radioactive labeled *i*th cation is studied in the presence of non-radioactive *i*th cation, there should be a competitive pattern similar to that shown in Fig. 2. On the other hand, reducing the *j*th-cation concentration to low values does not alter the indifference of the *i*th-ion entry to the *j*th-ion concentration.

Type 4: Apparent indifference. ($\tilde{K}_i \ll \tilde{K}_j$). When the *j*th-cation association constant is overwhelmingly larger than the *i*th-cation association (*i.e.*, $\tilde{K}_j \gg \tilde{K}_i$), *i*th-cation entry appears also to be indifferent to an increase in the concentration of the *j*th cation (Fig. 5). In this case the *i*th cation can enter only *via* the saltatory route. If the *j*th-cation concentration is reduced to a much lower range, the *i*th-cation will

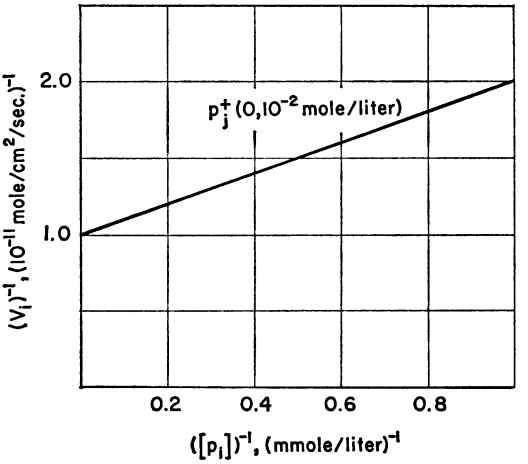

FIGURE 4 *Indifference: Theoretical effect of p_j^+ on the rate of entry of p_i^+, (V_i), into a fixed-charge system.* Reciprocal plot of values calculated from equation 15. Numerical values used were: $A = 10^{-10}$ (mole/second), $B = 10^{-7}$ (mole/second), $K_i^{ex} = 10^3$ (mole/liter)$^{-1}$, $K_j^{ex} = 1$ (mole/liter)$^{-1}$, exp $(-\Delta F_{ifi}^{\ddagger}/RT) = 10^{-4}$, exp $(-\Delta F_{ifi}^{\ddagger}/RT) = \exp \cdot(-\Delta F_{ifj}^{\ddagger}/RT) = 10^{-8}$, $C = D = 1$, $K_{ii}^{ex \cdot ex} = K_{ij}^{ex \cdot ex} = 10^{-1}$ (mole/liter)$^{-1}$.

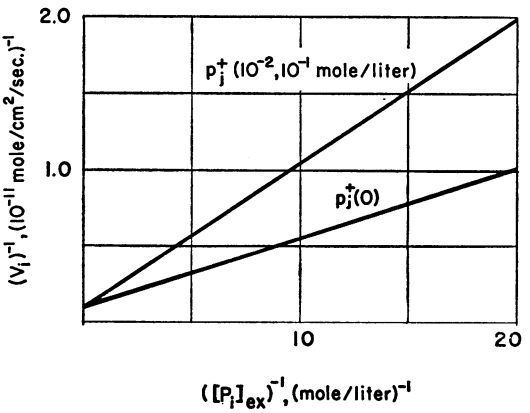

FIGURE 5 *Indifference: Theoretical effect of p_j^+ on the rate of entry of p_i^+, (V_i), into a fixed-charge system.* Reciprocal plot of values calculated from equation 15. Numerical values used were: $A = 10^{-10}$ (mole/second), $B = 10^{-7}$ (mole/second), $K_i^{ex} = 1$ (mole/liter)$^{-1}$, $K_j^{ex} = 10^4$ (mole/liter)$^{-1}$, exp $(-\Delta F_{ifi}^{\ddagger}/RT) = 10^{-8}$, exp $(-\Delta F_{ifi}^{\ddagger}/RT) = \exp (-\Delta F_{ifj}^{\ddagger}/RT) = 10^{-3}$, $C = D = 1$, $K_{ii}^{ex \cdot ex} = K_{ij}^{ex \cdot ex} = 1$ (mole/liter)$^{-1}$.

have more success occupying the surface sites and will enter to a greater or lesser degree *via* the adsorption-desorption route. One may then demonstrate inhibition of *j*th-cation on the *i*th-ion entry (Fig. 5).

Interactions of *Type 1* and *Type 2* can occur between the same ionic species (*e.g.*,

unlabeled K^+ ion inhibits K^{42}-labeled K^+-ion entry). Interactions of *Type 3* and *Type 4* can occur only between different ionic species.

Model IV: Model of cell membrane containing both fixed ionic sites and channels of polarized water.

This is a partial (and dismembered) view of the entire living cell as a fixed-charge system. Nevertheless, all theoretical predictions on the initial rate of entry presented in connection with the bulk-phase model (Model III) are fully applicable to Model IV; *i.e.*, a cell membrane containing fixed ionic sites and channels of polarized water.

MATERIALS AND METHODS

This paper presents experimental work performed both on living cells and on (non-living) models of the living cells. All chemicals used were of C.P. grade. Their sources and the sources of the isotopes have appeared elsewhere (18).

I. *Living Cells.*

All experimental results on living cells reported in this paper were obtained from sartorius muscles of leopard frogs (*Rana pipiens*, Schreber). The muscles were isolated either on the date of the experiment or on the previous day and stored overnight at 1°-4°C in a Ringer's phosphate solution, (for composition see reference 6, Appendix H).

For the study of the effect of H^+-ion concentration on the rate of ionic entry into frog muscle cells we chose the following buffers; pH 2.2-3.4, glycine-HCl; pH 3.8-5.8, succinic acid-NaOH; pH 6.2-7.8, NaH_2PO_4-Na_2HPO_4; pH 8.6-9.0, veronal-HCl; pH 8.6-11.6, glycine-NaOH (19). In these experiments, each test tube contained 18.4 ml of solution A,[3] 2.0 ml of one of the buffers mentioned, and 0.05 ml of neutralized K^{42} isotope solutions. The final K^+-ion concentration in this solution was 20 mmole/liter.

As a rule two or three sartorius muscles from different frogs were blotted on wet filter paper and introduced into wide test tubes (25 mm diameter × 100 mm) containing the experimental solution. The solution was stirred for a specified length of time by vigorous bubbling with 95 per cent O_2—5 per cent CO_2 mixture. At the same time the tubes were shaken in an aminco water bath, the temperature of which was controlled to within 0.05°C. In some experiments conducted at 0°C, the tubes were placed in a stationary bath containing an ice water mixture. The entire assembly was placed in a cold room, maintained at about 1°-4°C. Unless otherwise stated, 10 ml of the experimental solution were used in each test tube. In the experiments on Na^+-ion entry, only 3 to 5 ml of the experimental solution were used. Since the intracellular Na^+-ion concentration is very low, no significant change on external Na^+-ion concentration occurred within the duration of the experiment. At the end of incubation, the muscles were rapidly transferred to a non-radioactive Ringer's solution at 0°C, blotted dry, individually weighed, and introduced into lusteroid tubes containing 1 ml of 1 N HCl. The assay of radioactivity followed the procedure described elsewhere (18).

In determining the initial rate of entry of ions into cells, the duration of incubation and of washing are of considerable importance; investigations of this and other major procedural matter are described in detail below.

[3] A modified Ringer's solution containing 63 ml of 5 × 0.118 M NaCl, 100 ml of 0.118 M KCl with sucrose (see below), 5 ml of 0.08 M $CaCl_2$ 6 ml of 0.118 M $MgSO_4$, and 343.8 ml of water.

Tolerance Limits of Radioactivity.

Mullins (20) and Brooks (21) have both reported deleterious effects of radiation on the permeabilities of plant cells. The tolerable limit of K^{42} and Na^{24} isotopes for *Nitella* was 1 μc/ml. The low efficiency of Rb^{86} counting (6.4 per cent) in the γ-scintillation counter made it necessary to use relatively high radioactivity. We therefore employed Rb^{86} to test the tolerance of frog sartorius muscle cells. No appreciable difference in the Rb^+-ion permeability of frog sartorius muscles (or evidence of damage) could be detected after exposure to solutions containing as much as 5.0 μc/ml of Rb^{86}. These results are in harmony with high tolerance of animal cells toward radiation shown by Sheppard and Beyl (22). In actual experiments with Rb^{86} the concentration of the isotope was, as a rule, lower than 1 μc/ml; in the case of other isotopes it was much lower.

Procedure for Determining the Initial Rate of Entry into Cells.

(*a*) *Removal of extracellular radioactivity.* Isolated frog sartorius muscles were incubated in a stirred Ringer's solution containing labeled K^+ ion and maintained at a controlled temperature. After varying lengths of time, the muscles were tied at each end with thin surgical thread and fixed in a U-tube as shown in Fig. 6. The tissue was washed with a stream of non-radioactive Ringer's solution, maintained at 0°, while the radioactivity of the muscle was continually monitored by the scintillation well-counter-scaler assembly. The low temperature helped to minimize the loss of intracellular radioactivity as the extracellular radioactivity was washed away. Fig. 7 shows typical results from two out of a total of fifteen experiments performed. Each curve has two parts; an initial curved portion and a later straight portion. The curved portion becomes less and

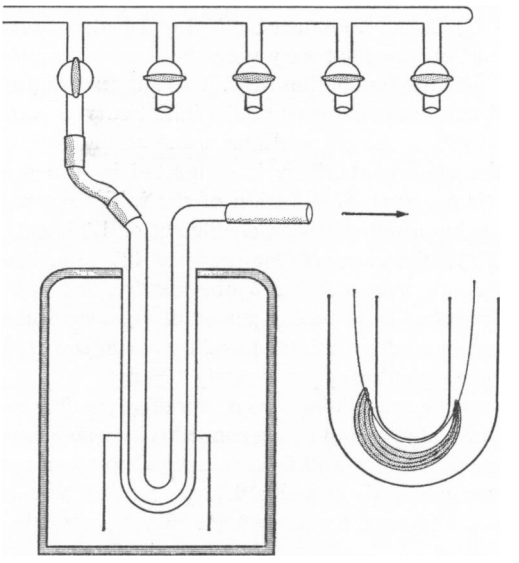

FIGURE 6 *Apparatus for continuous monitoring of efflux of radioactive isotope in living cells.* The glass U-tube was placed in the well of a γ-scintillation counter which continuously recorded the radioactivity within the muscle held in place with a piece of string (see inset), while a continuous stream of Ringer's solution flowed through the U-tube (arrow). The apparatus was designed so that several muscles could be observed simultaneously. The entire assembly was kept in a constant-temperature room.

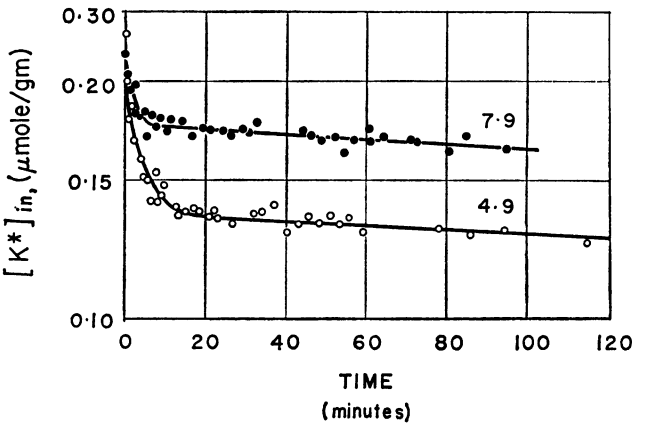

FIGURE 7 *Time course of K^{42} loss from frog sartorius muscles.* Muscles soaked briefly in K^{42}-tagged normal Ringer's solution. External labeled K^+-ion concentration was 2.5 mmole/liter. Ordinate represents the concentration of K^{42}-labeled K^+ ion (K*), in micromoles per gram of fresh tissue. The numbers, 7.9 and 4.9 in the figure refer to the number of minutes of soaking 0°C. Study made on the apparatus shown in Fig. 6. Each curve represents a single experiment.

less prominent with increasing time of incubation in the radioactive solution; after 68 hours of incubation (0°C), it can no longer be distinguished, (see reference 6, Fig. 11.2). The *slope* of the flat portion does not vary with the time of incubation, but its *absolute level* steadily increases with the incubation time. This suggests that the flat part represents the efflux of tagged ion within the cells, while the initial curved part represents, to a large extent, the radioactivity within the extracellular space and adhering to the surface of the cells and connective tissue elements. This is supported by the rough agreement found between the observed time course of diffusion of the initial portion of the curve, and a time course calculated using a self-diffusion coefficient of 1.25×10^{-5} cm²/second[4] and a minimum diffusion path in the extracellular space of 0.7 mm. The time for the radioactivity in the extracellular space to fall to 1 one hundredth of its initial value is of the order of 5 minutes. Thus, after a 10 minute period of vigorous washing in a non-radioactive Ringer's solution at 0°C the error introduced by entrapped radioactivity is negligible for a frog sartorius muscle weighing approximately 100 mg.

Besides occlusion in the extracellular space, another possible source of error exists; *i.e.*, the ions adsorbed on collagen and other connective tissue elements on the surface of the muscle cells and in the tendons and fascia attached to the muscle. On the average a well dissected frog sartorius muscle contains 9.1 per cent of such connective tissue (wet weight/wet weight) (see reference 6, Table 8.8). Fig. 8 shows the results of an experi-

[4] No data for the self-diffusion coefficient of K^+ ion at 0°C are available. On other occasions, the self-diffusion constant of Rb^+ ion in 0.1 M RbCl at 0°C (1.17×10^{-5} cm²/second) was determined in our laboratory by using a capillary method. The diffusion coefficient of Rb^+ ion at 25°C (in 0.1 M KCl) is 1.994×10^{-5} cm²/second. Using the temperature coefficient for Rb^+ ion diffusion between 0° and 25°C, we calculated the diffusion coefficient of K^+ ion at 0°C from the diffusion coefficient of K^+ ion at 25°C (2.135×10^{-5} cm²/second) (23), to yield the value of 1.25×10^{-5} cm²/second for K^+-ion diffusion at 0°C.

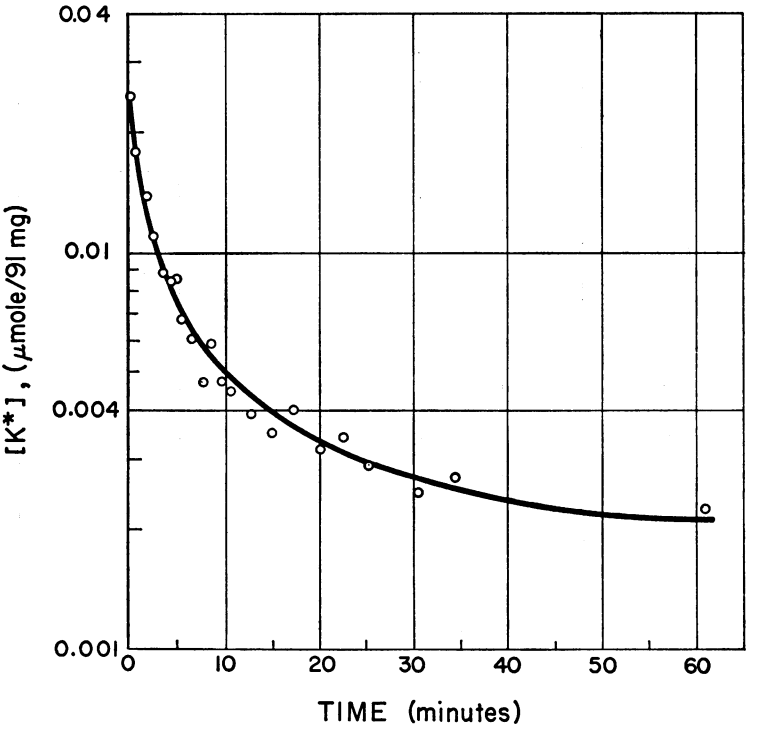

FIGURE 8 *Time course of K^{42} loss from connective-tissue elements.* Connective tissue elements from the region near the sartorius muscle of a frog were isolated and soaked in a normal Ringer's solution containing 2.5 mmole/liter of K^{42}-labeled K^+ ion for 6.9 minutes (0°C). Normal Ringer's solution at 0°C was used for washing. The data are presented on the basis of 91 mg of connective tissue, since this is the amount found in 1 gm of fresh sartorius muscle.

ment in which pieces of connective tissue elements dissected from the tendons and fascia surrounding the sartorius muscle were treated for a few minutes with Ringer's solution containing K^{42}-tagged K^+ ion and then washed in the U-tube as above. The concentration of tagged K^+ ion is expressed in moles per 91 mg of connective tissue, since 91 mg of connective tissue is present in each gram of frog sartorius muscle. Comparing the results with those shown in Fig. 7, one may conclude that for K^+ ion, the error introduced by adsorption onto connective tissue elements after 10 minutes of washing would amount to less than 3 per cent. The error is higher for Na^+ and Rb^+ ion because the uptake of these ions by muscle cells and by the connective tissue elements is of the same order of magnitude, whereas the uptake of K^+ ion by the muscle cells is higher than that by the connective tissue elements.

(*b*) *Time course of ionic entry into living cells.* Figs. 9 through 11 show that the experimentally determined time course of ionic entry is not logarithmic as would be anticipated on the basis of the membrane theory. There is usually a bend in the curve at about 1 hour. Thus, in order to obtain the true initial rate of entry into the tissue alone and avoid the bend at about 1 hour, the incubation time must be relatively short. How-

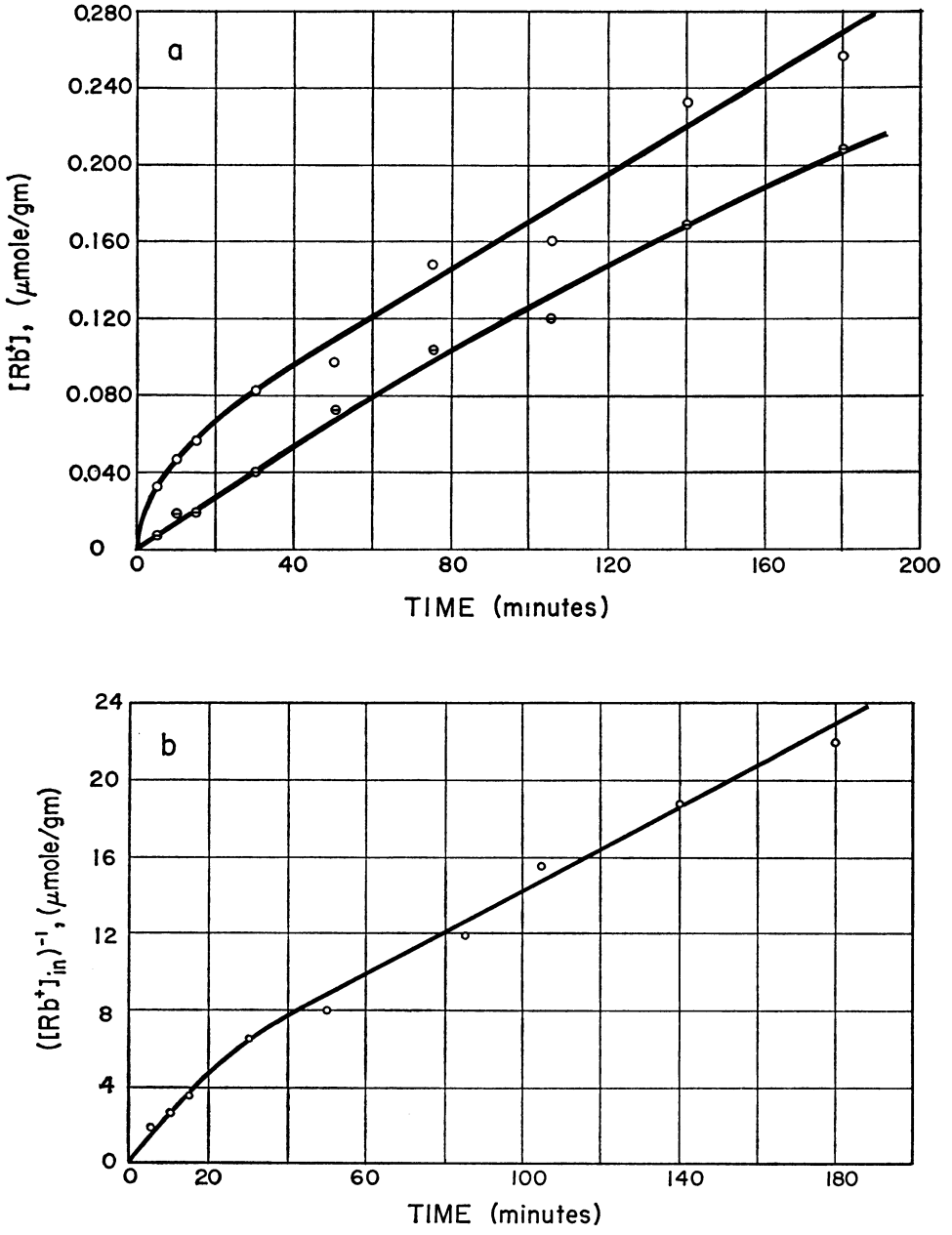

FIGURE 9 *Time course of labeled Rb^+-ion entry into frog sartorius muscles.* (*a*) Rb^+-ion concentration, 2.5 mmole/liter; temperature, 0°C. Upper curve represents blotted, but unwashed muscles; lower curve represents muscles washed for 10 minutes in a non-radioactive Ringer's solution (0°C). (*b*) Rb^+-ion concentration, 20 mmole/liter; temperature, 25°C. Muscles washed for 10 minutes at 0°C.

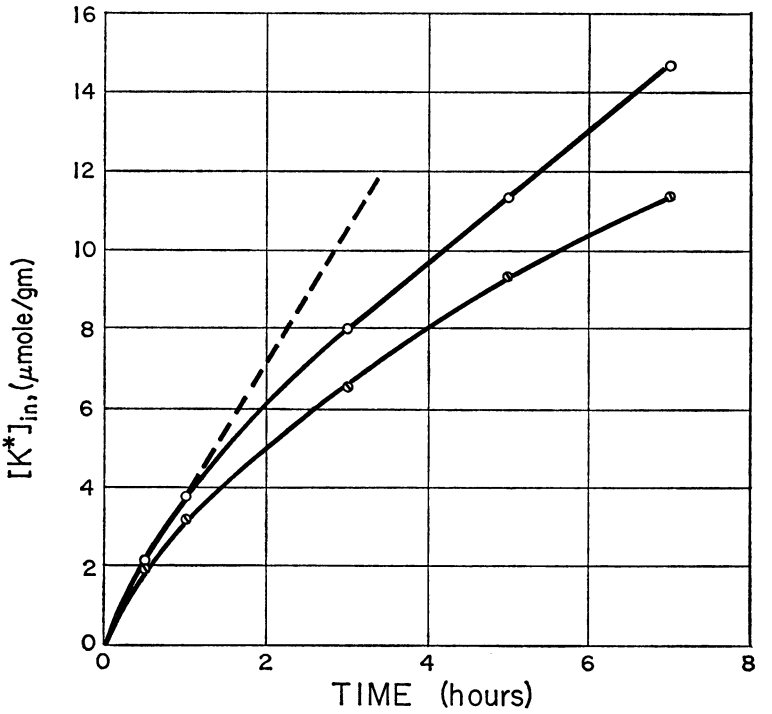

FIGURE 10 *Time course of labeled K^+-ion entry into frog sartorius muscles.* Upper curve, sartorius muscle only; lower curve, average of sartorius, semitendinosus, tibialis anticus longus, and iliofibularis. K^+-ion concentration, 2.5 mmole/liter; temperature, 0°C. Muscles assayed for radioactivity without washing. The dotted line indicates bend in time-course curve at about 1 hour.

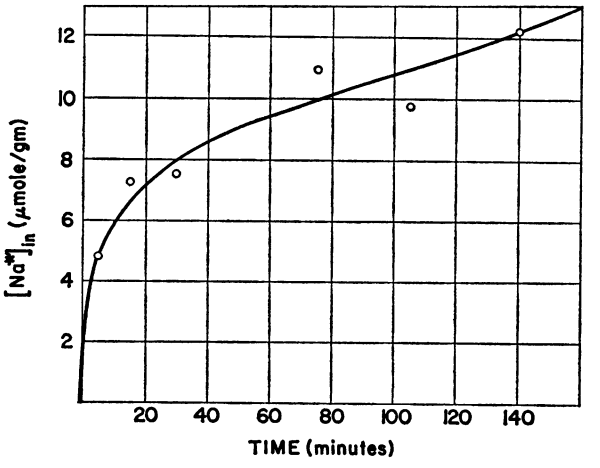

FIGURE 11 *Time course of Na^+-ion entry into frog muscles.* Sartorius muscles only. Soaking solution was normal Ringer's containing Na^{22} at 25°C. Muscles washed for 10 minutes at 0°C.

ever, this increases the relative significance of experimental errors originating from adsorption onto the more accessible connective tissues and from the loss of radioactivity from the cells during the washing process. The rate of Na^+-ion entry at both 0° and 25°C rapidly levels off after the initial 20 to 30 minutes; the best compromise involves soaking for 15 minutes, followed by washing for 5 to 10 minutes. For this ion the error introduced by the connective tissue elements for a 5 minute washing period is as much as 18 per cent. For Rb^+ ion, by combining a longer soaking time with a longer washing time (10 minutes), the connective tissue error can be reduced to 5 to 10 per cent (Table I).

TABLE I

EXPERIMENTAL ERRORS DUE TO ADSORPTION ON CONNECTIVE TISSUE ELEMENTS

Ion	Soaking		Washing		Initial rate of entry		Ion in connective tissue / Ion in whole tissue
	Time	Temp.	Time	Temp.	In muscle	In connective tissue	
	min.	°C	*min.*	°C	μM/gm/hr/mM*	μM/gm/hr/mM*	*per cent*
Na^+	15	0	5	0	0.082 ± 0.014 (*SD*) (*n* = 8)	0.162 (*n* = 2)	18
	15	30	5	0	0.149 ± 0.017 (*SD*) (*n* = 8)	0.225 (*n* = 2)	13.7
Rb^+	15	0	5	0	0.204 ± 0.05 (*SD*) (*n* = 8)	0.24 (*n* = 2)	10.7
	15	30	5	0	1.435 ± 0.29 (*SD*) (*n* = 8)	1.25 (*n* = 2)	8.0
	60	20	10	0	0.121 ± 0.20 (*SD*) (*n* = 12)	0.076 (*n* = 2)	6.3

*The number of micromoles that enter 1 gm of cell in an hour at an external ionic concentration of 1 mmole/liter.

The experiments reported in this paper, unless otherwise stated, involved a soaking time of 10 minutes to 1 hour, followed by a washing time of 10 minutes at 0°C.

Preserving the Normal Cell Volume. For the experimental solution used, extensive substitution of the NaCl in normal Ringer's phosphate solution by other salts such as KCl is necessary. In such solutions muscle cells do not maintain their physiological volumes but swell to varying degrees. To overcome this undersirable effect, we determined the amount of sucrose necessary to counteract completely the swelling action of 0.118 M solutions of KCl, RbCl, NH_4Cl, CsCl, and LiCl. The results appear in Fig. 12 in which the abscissa represents the number of milliliters of 0.472 M sucrose (4 × 0.118 M) solution that was included in 100 ml of 0.118 M KCl, RbCl, CsCl, NH_4Cl, or LiCl. The ordinate represents the per cent increase ($\Delta W/W > 0$) or decrease ($\Delta W/W < 0$) of weight seen in the isolated frog sartorius muscle after equilibration for 1 hour at room temperature. The point $\Delta W/W = 0$ corresponds to the number of milliliters of 4 × 0.118 M sucrose (given on the abscissa) necessary per 100 ml of salt solution to suppress its swelling effect. In all subsequent experiments were NaCl is extensively substituted by other salts, the necessary amount of sucrose is included according to the data of Fig. 12.

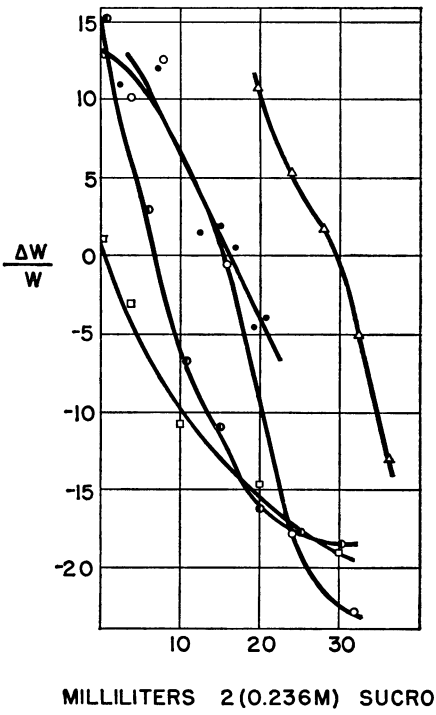

FIGURE 12 *Weight changes of frog sartorius muscles in salt-sucrose solutions.* Solutions contained 0.118 M KCl (△), RbCl (●), CsCl (○), NH_4Cl (half-filled circles) or LiCl (□), and varying concentrations of sucrose. Sucrose concentration is equal to $v/100 \times 0.472$ mmole/liter where v is the number of milliliters indicated on the abscissa. Ordinate represents per cent weight increase ($\Delta W/W > 0$) or decrease ($\Delta W/W < 0$).

All experimental solutions were modified Ringer's solutions as illustrated by Table II which shows the solutions prepared for an experiment studying the inhibitory effect of Rb^+ ion on the rate of K^+ (K^{42}-tagged) ion influx into frog muscle.

II. *Non-living Models of the Living Cell.*

We chose two types of inanimate fixed-charge systems to study as models of the living cell; cation exchange resin and sheep's wool. The procedures to be described were evolved from time course studies similar to those described for ion entry into frog muscles. The cation exchange resin was of the sulfonated polystyrene type in the form of thin sheets (nalfilm 1) from the National Aluminate Co., Chicago. They were cut accurately into small strips of uniform dimension (3.81 cm long and 0.8 cm wide). Five pieces, chosen at random, weighed 26.5, 26.7, 24.8, 24.8, and 25.1 mg respectively (average = 25.6 mg). The average thickness of these sheets was 84 μ, which is of the same order of magnitude as the diameter of muscle fibers (60 to 89μ) (see reference 6, Table 8.7) and wool fibers (20 to 40μ) (24). Their uniformity in thickness and ease in handling made these sheets far superior for the present purpose to exchange resin beads. For studies on the rate of ion entry, as a rule, one resin strip was vigorously shaken in 25 ml of the experimental solution for 3 to 4 minutes, followed by rinsing for 10 seconds in distilled water (0°C). After blotting, it was placed in a lusteroid tube for counting. We found that the radiation recorded from a sheet of nalfilm rolled onto a ring and placed at the bottom of a lusteroid counting tube is, within experimental error, identical with that recorded after the resin strip has been wet-ashed in concentrated H_2SO_4 and placed in the same lusteroid counting tube for assay.

Two batches of sheep's wool, gifts from J. Webb and Co., Inc., Philadelphia, and

TABLE II

AN EXAMPLE OF THE COMPOSITION OF A SET OF EXPERIMENTAL SOLUTIONS

Solution No.	Mixture A* 0.118 M	KCl‡ 0.118 M	RbCl 0.118 M§	Sucrose 0.472 M	Water	$CaCl_2$ 0.0846 M
Q_1	60.5	2.0	0	28.5	27.2	1.0
Q_2	60.5	2.5	0	28.3	26.9	1.0
Q_3	60.5	3.33	0	28.2	26.2	1.0
Q_4	60.5	5.0	0	27.9	24.9	1.0
Q_5	60.5	10.0	0	26.8	20.9	1.0
Q_6	60.5	20.0	0	24.7	13.0	1.0
R_1	60.5	2.0	4	26.5	25.2	1.0
R_2	60.5	2.5	4	26.3	24.9	1.0
R_3	60.5	3.33	4	26.2	24.2	1.0
R_4	60.5	5.0	4	25.8	22.9	1.0
R_5	60.5	10.0	4	24.8	18.9	1.0
R_6	60.5	20.0	4	22.6	11.1	1.0
S_1	60.5	2.0	15	20.9	19.8	1.0
S_2	60.5	2.5	15	20.8	19.4	1.0
S_3	60.5	3.33	15	20.7	18.7	1.0
S_4	60.5	5.0	15	20.4	17.3	1.0
S_5	60.5	10.0	15	19.3	13.4	1.0
S_6	60.5	20.0	15	17.2	5.5	1.0
T_1	60.5	2.0	25	15.9	14.8	1.0
T_2	60.5	2.5	25	15.8	14.4	1.0
T_3	60.5	3.33	25	15.7	13.7	1.0
T_4	60.5	5.0	25	15.3	12.4	1.0
T_5	60.5	10.0	25	14.3	8.4	1.0
T_6	60.5	20.0	25	12.2	0.5	1.0

*Mixture A contains 54.0 ml of 0.118 M NaCl; 1.2 ml of 0.118 M $MgSO_4$, 2.0 ml of 0.118 M NaH_2PO_4, 1.0 ml of 0.118 M Na_2HPO_4, and 2.3 ml of 0.118 M $NaHCO_3$.

‡K^{42}-tagged KCl solution.

§0.118 M RbCl containing 8.0 mmole/liter sucrose.

from Hemphill Co., Inc., Philadelphia, were cleaned and defatted according to the procedure of Steinhardt *et al.* (25). As a rule 30 mg of wool were placed in 25 ml of experimental solution in a wide test tube and shaken in an aminco constant temperature bath. Connection of the tubes to a vacuum line helped to remove the air trapped around the wool. After a few minutes of incubation, the wool was removed from the tubes, blotted dry on filter paper, and placed on a fritted glass filter (25 ml coarse grade) connected to a vacuum line through a suction bottle. With the aid of strong suction, three 10 ml portions of ice cold distilled water were allowed to flow rapidly through the wool, removing all adhering experimental solution. After a final blotting on filter paper, the wool was placed at the bottom of a lusteroid tube and its radioactivity assayed with a γ-scintillation counter. The counts thus obtained for Cs^{134} in wool were comparable to

those given by the same amount of Cs^{134}-containing wool after dissolution in 1 ml of concentrated NaOH, and it was unnecessary to introduce a correction factor.

RESULTS

I. Experiments on Living Cells.

Effects of alkali-metal ions on the rate of entry of alkali-metal ions. (*a*) *Competition.* Fig. 13 shows the competitive effects of Rb^+, Cs^+, and non-

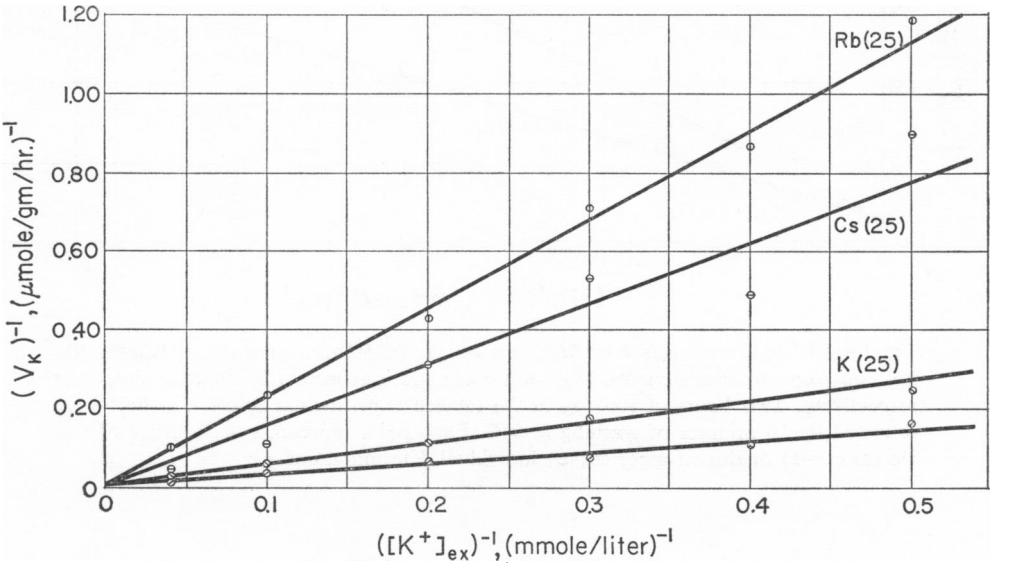

FIGURE 13 *Inhibitory effect of 25 mmole/liter of Rb^+, Cs^+ and non-labeled K^+ ion on the initial rate of entry of labeled K^+ ion into frog sartorius muscles.* Lowest, unlabeled curve represents the rate of K^+-ion entry with no added competing ion. Muscles, soaked for 30 minutes at 24°C, followed by 10 minutes of washing at 0°C. Each point represents a single determination on two sartorius muscles.

labeled K^+ ions on the rate of entry of K^{42}-labeled K^+ ion into frog sartorius muscle at 25°C. Figs. 14 and 15 show the similar competitive effects of Mg^{++} and Cs^+ ions on Rb^+ ion entry at 0°C.

Calculated on the basis of equation 3 or the simplified version of equation 4 (considering only the carrier mechanism), or of equation 5 (considering only doublet entry), the data yield the following apparent association constant (0°C) in $(\text{mole/liter})^{-1}$; 46 for Mg^{++} ion, 39 for Rb^+ ion, and 52 Cs^+ ion.[5] At 25°C they are; 42 for K^+ ion, 183 for Cs^+ ion, and 296 for Rb^+ ion.

[5] These values are different from those given earlier for frog muscles (5, 6). In the present study we performed experiments on frog sartorius muscles alone using short periods of soaking (30 minutes), whereas in the earlier work we used four small muscles (sartorius, semitendinosus, tibialis anticus longus, and iliofibularis) as a group, and a longer period of soaking (1 to 4 hours).

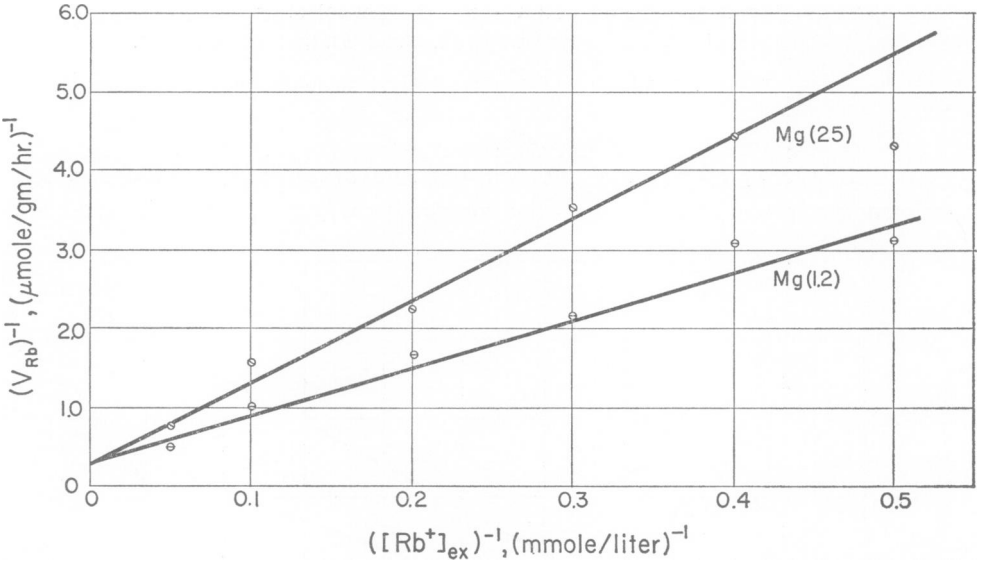

FIGURE 14 *Inhibitory effect of Mg^{++} ion on the initial rate of entry of labeled Rb^+ ion into frog sartorius muscles.* Mg^{++}-ion concentrations were 1.2 and 25 mmole/liter respectively. Two hours of soaking in the labeled experimental solution at 0°C were followed by 10 minutes of washing at 0°C. Each point represents the average of two (lower curve) or three (upper curve) individual determinations.

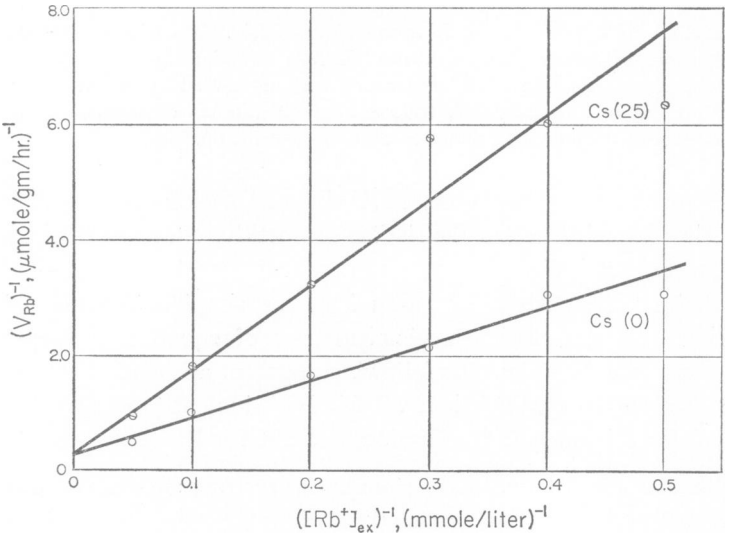

FIGURE 15 *Inhibitory effect of 0 and 25 mmole/liter of Cs^+ ion on the initial rate of entry of labeled Rb^+ ion into frog muscles.* Experimental details the same as in Fig. 14.

(*b*) *Facilitation.* Fig. 16 shows the effect on Rb^+ ion entry of increasing the concentration of KCl from 2.5 to 10 mmole/liter. Unlike the inhibiting effect of Rb^+-ion on K^+ entry, the effect of K^+ ion on Rb^+ entry is facilitory; the rate of Rb^+-ion entry increases with increasing K^+-ion concentration. Fig. 17 shows that the facilitory action of KCl is due to K^+ ion and not to the Cl^- ion, since 10 mmole/liter K-phosphate produced essentially the same facilitation as 10 mmole/liter KCl.

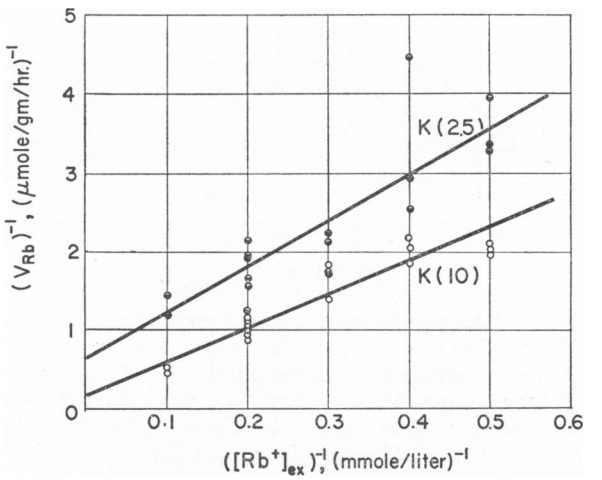

FIGURE 16 *Facilitory effect of K^+ ion on the rate of entry of labeled Rb^+ ion into frog sartorius muscles.* K^+-ion (as chloride) concentrations were 2.5 and 10 mmole/liter. Each point represents a determination on a single muscle. Muscles soaked 30 minutes at 0°C followed by 10 minutes of washing at 0°C.

Fig. 18 demonstrates the similar facilitory effect of Na^+ ion on the rate of entry of Rb^+ ion at 25°C. In this case, the Na^+ salt was used as the sulfate. Elsewhere, the facilitory action of Na^+ ion as the chloride on Rb^+-ion entry has been shown (see reference 6, Fig. 11.18); the soaking time, however, was much longer (3.5 hours) and the temperature was 0°C. Other experiments (not shown) demonstrated that the facilitory action of K^+ on Rb^+-ion entry also persists when the soaking time is prolonged to 3.5 hours (0°C).

(*c*) *Absence of demonstrable effect.* Fig. 19 shows that Li^+ ion has either no effect or a very small facilitory effect on Rb^+-ion entry.

Fig. 20 shows the effect of K^+ ion on the rate of entry of Na^+ ion. An increase in the competing K^+-ion concentration from 30 to 100 mmole/liter, does not effect the rate of Na^+-ion entry. However, reducing the K^+-ion concentration to 2.5 mmole/liter indicates distinct competition. Further reduction of the external K^+-ion concentration did not increase but actually slightly decreased the rate of Na^+-ion entry.

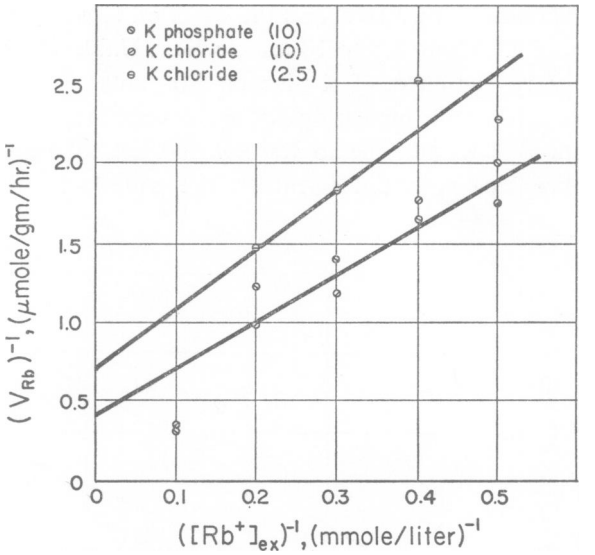

FIGURE 17 *Essential independence of the facilitory effect of K salt on the nature of the anion.* The facilitory action of K^+ ion on Rb–ion entry is the same whether the K^+ ion is added as the chloride or as the phosphate. There was thirty minutes of soaking at 0°C for all muscles except those with the highest Rb^+–ion concentration (10 mmole/liter), which were soaked for 15 minutes to avoid the change in the rate of entry (see Fig. 9 *b*). Washing was in normal Ringer's solution at 0°C for 10 minutes. Each point represents a single determination on a single sartorius muscle (Cl) or on two sartorius muscles (PO_4).

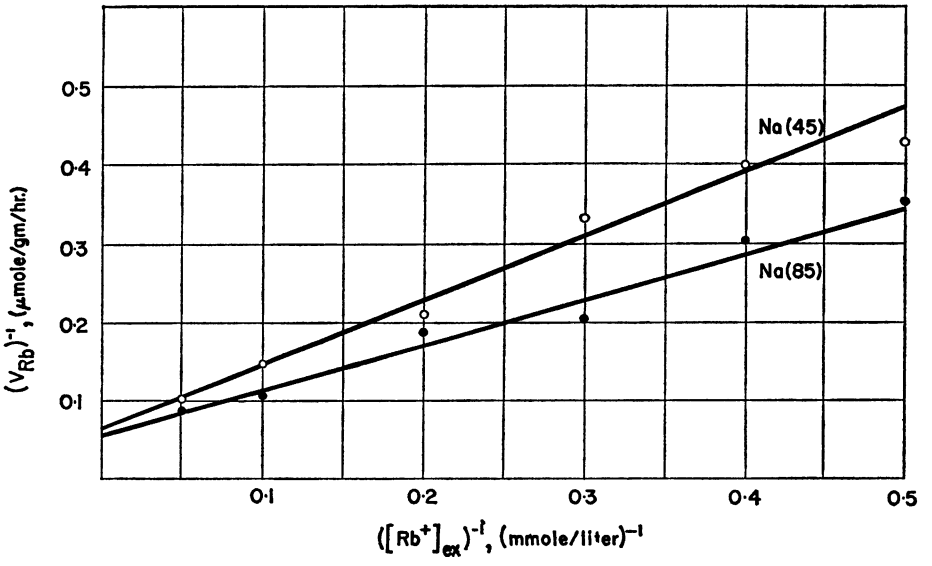

FIGURE 18 *Facilitory action of Na^+ ion on the rate of entry of labeled Rb^+ ion into frog sartorius muscles.* Na^+ ion added as sulfate. Thirty minutes of soaking at 25°C were followed by 10 minutes of washing (0°C). Each point represents the average of three individual determinations.

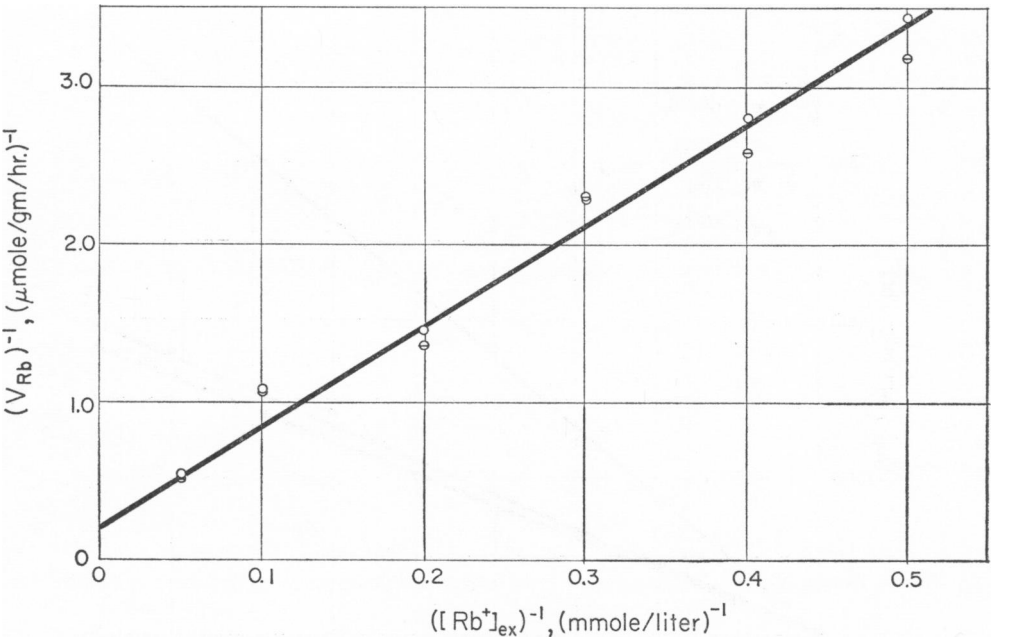

FIGURE 19 *Apparent lack of effect of Li^+ ion on the rate of Rb^+ ion entry into frog sartorius muscles cells.* Soaking in experimental solution for 2 hours at 0°C was followed by 10 minutes of washing at 0°C. Each point represents the average of three individual determinations. Li^+-ion concentrations were zero (○) and 25 mmole/liter (⊖) respectively.

Effect of H^+ ion on the rate of entry of K^+ ion. Fig. 21 shows an example of the three series of experiments conducted on the effect of pH on the rate of K^+-ion entry (25°C). From pH 6–10.4, the rate of K^+-ion entry is virtually constant at approximately 42 mM per gram of cells per hour. We obtained somewhat higher plateau values in two other series. Below pH 6 the rate of K^+-ion entry declines, flattening off again at about pH 3.[6] The midpoint of the declining curve corresponds approximately to a pH of 4.6–4.7

II. *Experiments on Inanimate Fixed-Charge Systems.*

Ion exchange resins. Fig. 22 shows reciprocal plots of the effects of 40 mmole/liter of Li^+, Na^+, K^+, and Cs^+ ions at 25°C on the rate of entry of Cs^{134}-labeled Cs^+ ion into sulfonate exchange resin film strips (in H^+-ion form). The results show distinct competition.

Calculated on the basis of equation 3 or the simplified version of equation 4 or equation 5 (see above), one obtains an apparent association constant for Cs^+ ion

[6] We confirmed an earlier report (26) of the instability of frog sartorius muscles at pH values lower than 4.5 but proved it to be due to the combined action of H^+ and acetate ions. We averted this deleterious effect by using glycine and succinate buffers.

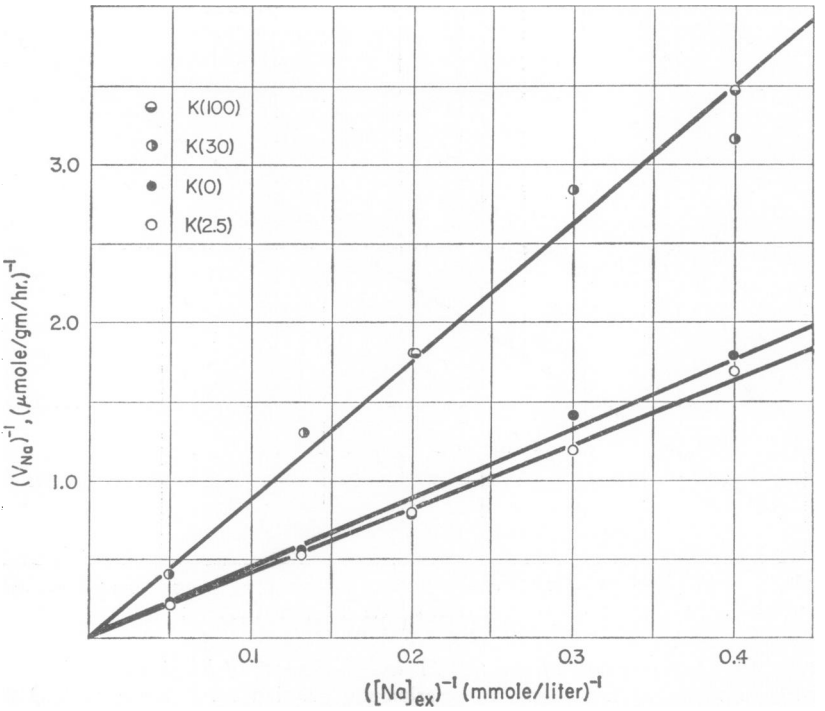

FIGURE 20 *Effect of various concentrations of K^+ ion on the initial rate of entry of Na^+ ion into frog sartorius muscles.* Increasing K^+-ion concentration from 30 mmole/liter to 100 mmole/liter causes no apparent effect on the rate of Na^+ ion entry, while reduction from 30 mmole/liter to 2.5 mmole/liter causes an increased rate of Na^+-ion entry. Fifteen minutes of soaking at 25°C were followed by washing for 10 minutes at 0°C. Each point represents average of three individual determinations.

(as entrant ion) equal to 235 (mole/liter)$^{-1}$. As competing ions the apparent association constants for Li^+, Na^+, K^+, and Cs^+ ion are respectively; 65, 123, 164, and 237 in (mole/liter)$^{-1}$.

Sheep's wool. Fig. 23 shows reciprocal plots of the effects of K^+ ion on the rate of entry of labeled Cs^+ ion into sheep's wool at 25°C. The results show, as in the case of ion exchange resins, distinct competition of K^+-ion with Cs^+-ion entry.

Again calculated on the basis of equation 3 or the simplified version of equation 4 or equation 5 (see above) one obtains an apparent association constant in (mole/liter)$^{-1}$ of 18 for Cs^+ ion and 37 for K^+ ion.

DISCUSSION

In an earlier section we presented four theoretical models; Model I (impermeable membrane-carrier model) is well known, Model III (bulk-phase association-induction model) has also been presented before; Model II (leaky membrane-carrier) and Model IV (fixed-charge bearing membrane with aqueous channels)

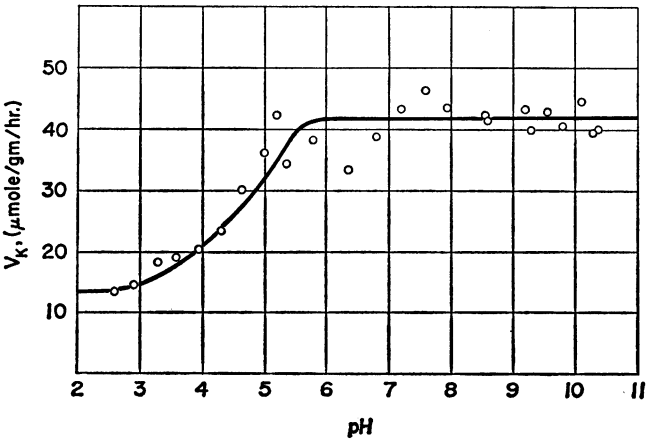

FIGURE 21 *Effect of pH on the initial rate of entry of labeled K^+ ion into frog sartorius muscles.* Labeled K^+–ion concentration was 20 mmole/liter; concentration of phosphate buffer was 10.8 mmole/liter; of the glycine, succinate, and veronal buffers, 5.4 mmole/liter. Muscles isolated on the previous day and kept overnight at 2°C in Ringer's solution. Fifteen minutes of soaking at 25°C were followed by 10 minutes of washing at 0°C pH of experimental solution measured after the experiment. Each point represents the average of three individual determinations.

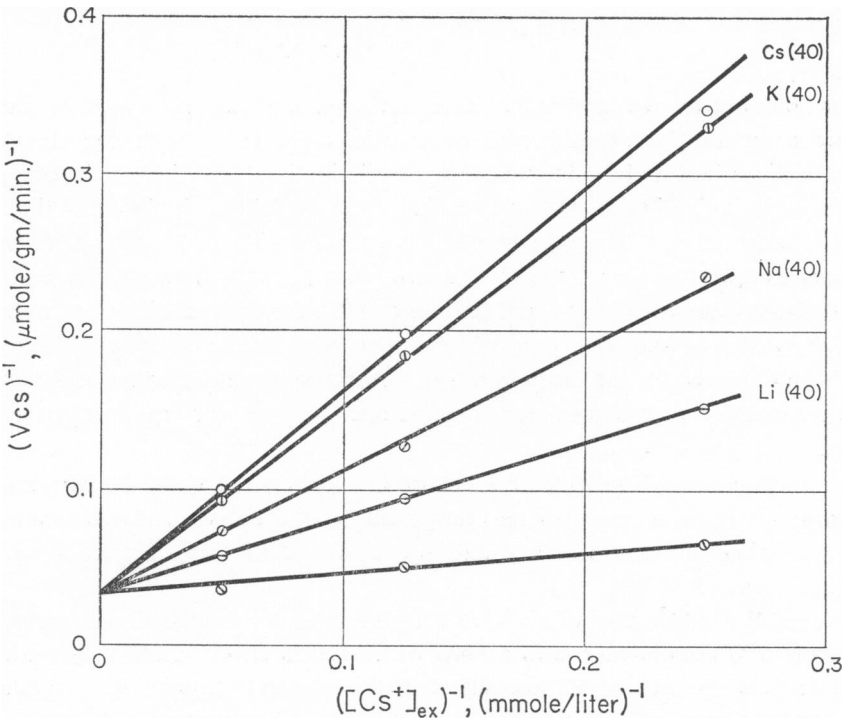

FIGURE 22 *Effects of CsCl, KCl, NaCl, and LiCl on the initial rate of entry of labeled Cs^+ ion into ion exchange resin sheets.* Nalfilm-1 strips soaked for 2 minutes at 5°C in an experimental solution containing (approximately) 2.5 mmole Tris buffer at pH 7.0, the labeled entrant ion and non-labeled ion (40 mmole/liter) as indicated in the figure. Strips washed for 10 seconds in cold distilled water (0°C) before counting.

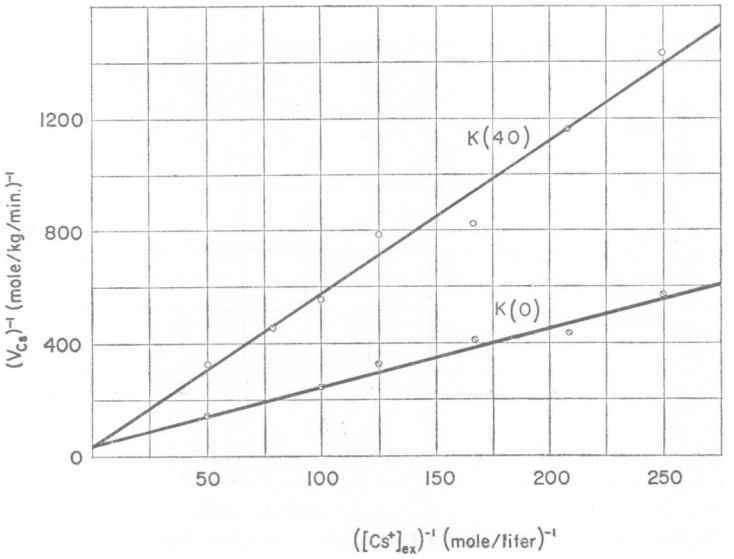

FIGURE 23 *Inhibitory effect of KCl on the initial rate of entry of labeled Cs^+ ion into sheep's wool.* Wool soaked for 4 minutes in an experimental solution (25°C) containing labeled Cs^+ ion, non-labeled K^+ ion (0 and 40 mmole/liter), and approximately 2.5 mmole/liter of Tris buffer at pH 7.0.

are not new, but to our knowledge, have not been explicitly presented before. Let us now compare the experimental observations presented with the theoretical characteristics of each of the four models. By eliminating those that are incompatible with the experimental facts, we may recognize the model that is closest to the truth.

Competition. The experimental data shown in Figs. 13, 14, and 15 demonstrate competition between Rb^+, Cs^+, and K^+ ion (25°C), between Cs^+ and Rb^+ ion (0°C), and between Mg^{++} and Rb^+ ion (0°C) for the same sites or carriers on the surface of frog sartorius muscles. As mentioned earlier such competition has often been observed for ion entry into frog sartorius and other small muscles (5, 6). These competition phenomena, considered alone, support with equal weight all four models.

Indifference. The lack of effect of Li^+ ion on the entry of Rb^+ ion into frog sartorius muscles can also be interpreted on the basis of all four models as being due to the much smaller association constant of Li^+ ion, $\tilde{K}_{Li}$, in comparison with that of the Rb^+ ion, $\tilde{K}_{Rb}$.

However, the indifference of Na^+-ion entry to an increase of K^+-ion concentration from 30 to 100 mmole/liter is in accord with Models II, III, and IV but not with Model I; thus the lack of K^+ ion effect in this concentration range suggests that whatever K^+ ion does to Na^+-ion entry, this effect has reached saturation at 30 mmole/liter. In the case of Model I this would mean complete exclusion of Na^+ ion

from the inward carrier. However, according to Model I the continuous lipoid membrane is impermeable to ions, and *total* inhibition of Na^+-ion entry at 30 to 100 mmole/liter K^+-ion concentration is predicted. This prediction is not borne out by the experimental observations which show that under these condition Na^+-ion entry is decreased but is still far from being zero.

Facilitation. Fig. 13 shows that Rb^+ ion competitively inhibits K^+-ion entry. Thus according to Model I (*i.e.*, equation 3) and Model II (*i.e.*, equation 4) K^+ ion must either inhibit or have no effect on Rb^+-ion entry; under no condition would these models predict facilitation of Rb^+-ion entry by K^+ ion (or by Na^+ ion). The fact that such facilitation is observed for Rb^+-ion entry (Figs. 16, 17, and 18) is not consistent with either Model I or Model II. However, the data are in accord with Model III and Model IV.

pH effect. Since the demonstration of the very low surface tension of the living cells in an aqueous environment by Harvey, Collander, Cole, and others, a concensus seem to have emerged; the outer surface of the cell is proteinaceous in nature and contains ionic groups (8, 27–30). From other experimental evidence we have reached the conclusion that the ionic sites on the cell surface are primarily, if not exclusively, *anionic* (reference 6, section 10-4). In other words, the cell surface is, in fact, an anionic fixed-charge system and, in this respect, resembles ion exchange resin and dried oxidized collodion. As such, that living muscle cells show competitive ionic entry similar to these models is not surprising.

The competitive ionic entry into the sulfonate type of exchange resin and into sheep's wool demonstrates that competition is the consequence of the possession of fixed anionic sites, regardless of the specific nature of these sites. In muscle cells the possible anionic groups include sulfonic acid groups on the chondroitin sulfate of the surface connective tissues, phosphate groups in phospholipids, or polyphosphate groups. The study of the effect of pH on K^+-ion entry (Fig. 21) shows that the surface anionic group involved has a pK value of 4.6. These results rule out sulfonic acid groups which have a pK value of 2 (see reference 31); they also rule out the phosphate or polyphosphate groups which, as a rule, have a pK value between 6.1 and 6.5. However, it does correspond to the known pK values of β- and γ-carboxyl groups of proteins; *i.e.*, 4.6 to 4.7 (see reference 32, Table I).

Conclusion. The experimental data presented do not support either Model I or Model II but do support with equal weight Model III and Model IV, if one considers permeability phenomena alone. There are, of course, two ways of looking at Model IV: (*a*) that this fixed-charge–bearing membrane forms the outer boundary of a cell containing similar fixed charges throughout its bulk phase; this view is not different from Model III; (*b*) that this fixed-charge–bearing membrane is the membrane of the membrane theory, originally postulated by Pfeffer (33) and by Overton (1).

This second view, in categorically rejecting the concept of significant ionic asso-

ciation in the cytoplasm, is, in the first place, inconsistent; if the β- and γ-carboxyl groups of the surface proteins are capable of a high degree of selective adsorption of alkali metal cations, the bulk-phase β- and γ-carboxyl groups cannot be considered incapable of the same (see reference 18 for direct evidence *for* ionic adsorption on the β- and γcarboxyl groups of cytoplasmic proteins).

This second view, in assigning the ion binding sites to the surface-fixed charges, eliminates from consideration carriers or pumps. Without the aid of these hypothetical devices and with no specific ionic adsorption within the cytoplasm, this model cannot maintain the well known asymetrical distribution of ions and other solutes across the cell membrane (6).

Thus, within the limit of the authors' knowledge, Model III is the only self-consistent model which agrees with all the experimental observations presented in this paper.

APPENDIX

Whereas the general equation applies to the case of cationic entry into a fixed anionic system, as well as to the case of anionic entry into a fixed cationic system, for simplicity we shall confine our attention to cationic entry into a fixed anionic system (see reference 6, chapter 11). The following equations were derived on the basis of the "Theory of Absolute Reaction Rate" (34–37) as applied to diffusion (34, 38–40). In the case of the saltatory migration,

$$(V_i^{\text{inw}})_{\text{sal}} = \lambda_{\text{sal}}^2 \frac{kT}{h} A_{\text{sal}} \tau_i [p_i^+]_{\text{ex}} \frac{(p.f.)_i^{\ddagger}}{(p.f.)_i^{fr}} \exp(-\epsilon_i/RT). \tag{6}$$

where λ_{sal} is the distance between two successive equilibrium positions and k and h are the Boltzmann and Planck constants respectively. T is absolute temperature; A_{sal} is the total surface area for the saltatory entry of the ith ion; τ_i is the transmission coefficient (34). $[p_i^+]_{\text{ex}}$ is the external ith cation concentration, $(p.f.)_i^{\ddagger}$ is the partition function of the ith cation in its activated state *via* the saltatory route; ϵ_i is the corresponding activation energy for the ith cation; $(p.f.)_i^{fr}$ is the partition function of the ith free ion. (To avoid confusion, we have omitted another theoretically possible saltatory route in which the ith cation enters as an ion pair with a free external anion.) For the doublet entry, one has

$$(V_i^{\text{inw}})_{\text{dbt}} = \lambda_{\text{dbt}}^2 \frac{kT}{h} \tau_{if} l_{if} \{f^-\} [X_i^{\text{ex}}] \frac{(p.f.)_{if}^{\ddagger}}{(p.f.)_i^{\text{ads}}} \exp(-\epsilon_{if}/RT). \tag{7}$$

λ_{dbt} is the distance between two successive equilibrium positions for the doublet migration; l_{if} is a libration factor; it measures the fraction of the ith external cation-fixed anion complex with the cation oriented toward the inside of the cell (see below). The fixed anionic site concentration, in moles per cm,^{2} is represented as $\{f^-\}$; we assume that these fixed anions are all of the same kind. $(p.f.)_i^{\text{ads}}$ and $(p.f.)_{if}^{\ddagger}$ are the partition functions of the ith adsorbed cation and the ith activated cation-fixed site complex respectively in a doublet migration. ϵ_{if} is the corresponding activation energy; and τ_{if} is the transmission coefficient of the ith cation in a doublet migration. If there are altogether n types of cations in the

system and X_i^{ex} is the mole fraction of the surface, fixed anionic site occupied by the ith (subscript) external (superscript) cation, then,

$$[X_i^{ex}] = \frac{K_i^{ex}[p_i^+]_{ex}}{1 + \sum_{s=1}^{n} K_s^{ex}[p_s^+]_{ex} + \sum_{s=1}^{n} K_s^{ins}[p_s^+]_{ins}}, \tag{8}$$

where s is the general symbol of the n monovalent cations in the system, including the ith and jth. $[p_s^+]_{ex}$ and $[p_s^+]_{ins}$ refer to the sth cation in the external solution and in the interstitial water respectively. K_s^{ex} and K_s^{ins} are the association constants of the sth external and interstitial cation on the fixed anionic site respectively. In addition,

$$K_s^{ex} = \frac{(p.f.)_s^{ads \cdot ex}}{(p.f.)_s^{fr}} \exp(-\Delta E_s^{ex}/RT), \tag{9}$$

and

$$K_s^{ins} = \frac{(p.f.)_s^{ads \cdot ins}}{(p.f.)_s^{ins}} \exp(-\Delta E_s^{ins}/RT). \tag{10}$$

where $(p.f.)_s^{ads \cdot ex}$, $(p.f.)_s^{ad \cdot ins}$, $(p.f.)_s^{ins}$, and $(p.f.)_s^{fr}$ are the partition function of the sth adsorbed from outside and inside the cell, interstitial, and free ions respectively and ΔE_s^{ex} and ΔE_s^{ins} are the association energies (adsorption energies) of the sth external and sth interstitial cation on the surface, fixed anionic sites respectively.

We may again divide the triplet route into two classes, one of which is designed as the "billiard" type, in which, as is shown in Fig. 24, the adsorbed ith external cation first revolves around the fixed anion. The ith cation-fixed anion complex then forms a triplet with another external sth cation, before the final dissociation and entry of the ith cation into the fixed-charge system. We may name a second type the "pinwheel" type in which an interstitial sth cation from within the fixed-charge system forms a triplet with a fixed anion-ith external cation pair. The triplet then spins around, resulting in a configuration in which the external ith cation is now on the inside of the fixed anion and the sth cation is on the outside; the external ith cation then dissociates and enters the cell interior. To simplify the presentation in his paper, we shall limit the present discussion of this triplet route to the billiard type. In this case,

$$(V_i^{inw})_{tpt} = \lambda_{tpt}^2 \frac{kT}{h} \tau_{isf} \{f^-\} [X_i^{ex}] \left(\sum_{s=1}^{n} l_{isf} [X_{is}^{ex \cdot ex}] \frac{(p.f.)_{isf}^{\ddagger}}{(p.f.)_{is}^{ads}} \exp(-\epsilon_{isf}/RT) \right). \tag{11}$$

where λ_{tpt} is the distance between two successive equilibrium positions for the triplet route, τ_{isf} is the transmission coefficient for the ith cation in a triplet migration, $(p.f.)_i^{ads}$ is the partition function of the is triplet (non-activated); $(p.f.)_{isf}^{\ddagger}$ and ϵ_{isf} are the partition function and activation energy of the is triplet in its activated state respectively. l_{isf} is the libration factor for the billiard type of entry; it measures the percentage of the ith external ion-fixed ion complex which has the ith cation oriented on the inside of the fixed anions. It may represent either a steady-state ratio or an equilibrium distribution ratio, depending on the relative rate of successful dissociation. $[X_{is}^{ex \cdot ex}]$ is the mole fraction of the ith external cation-fixed anion complex which exists in the ith external cation-fixed anion-sth external cation state. And,

$$[X_{is}^{ex \cdot ex}] = \frac{K_{is}^{ex \cdot ex}[p_s^+]_{ex}}{1 + \sum_{s=1}^{n} K_{is}^{ex \cdot ex}[p_s^+]_{ex}}. \tag{12}$$

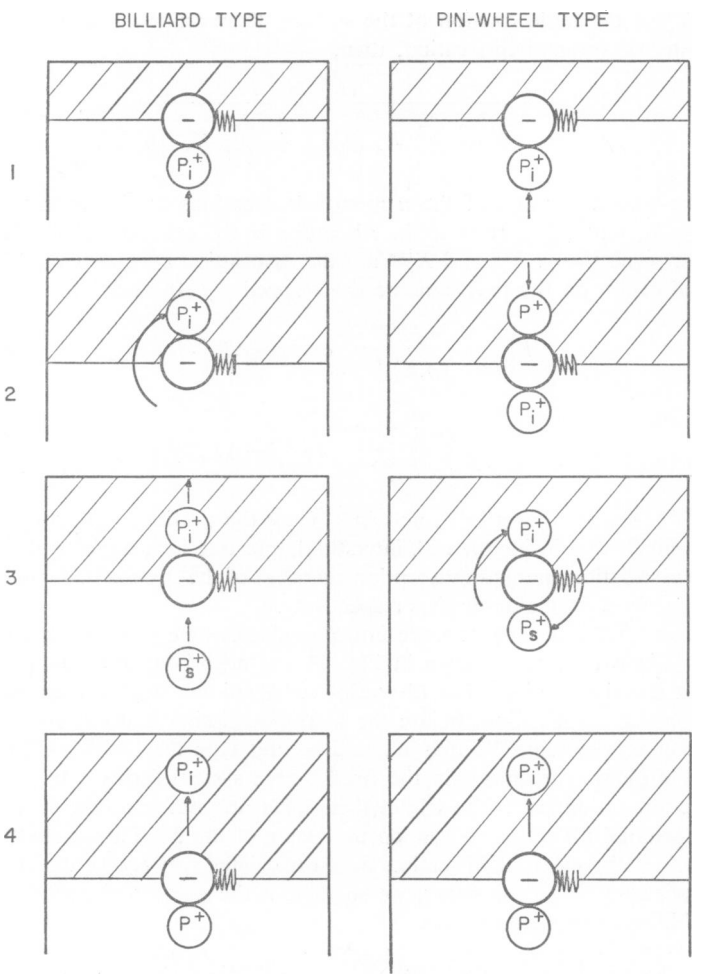

FIGURE 24 *Diagrammatic illustration of the "billiard" (left) and the "pin-wheel" (right) modes of entry of* p_i^+. These are two possible varieties of the triplet adsorption-desorption route, so named because the event involves three ions; *i.e.*, the fixed anion and two free cations. The difference between the "billiard" and the "pin-wheel" types lies in the origin of the second cation p_s^+. In the "billiard" type, p_s^+ is also from the external solution; in the "pin-wheel" type, p_s^+ is an ion from within the fixed-charge system (shaded area). The symbols represent hydrated ions in which, for simplicity, the associated water molecules do not appear.

$K_{is}^{ex \cdot ex}$, the association constant of the *is* triplet whose concentration is $[p_i^{ex} \cdot f^- \cdot p_s^{ex}]$ is described by the following relations:

$$K_{is}^{ex \cdot ex} = \frac{[p_i^{ex} \cdot f^- \cdot p_s^{ex}]}{\{f^-\}[p_i^+]_{ex}[p_s^+]_{ex}}. \tag{13}$$

Since the fixed anion has no freedom of motion, its partition function is unity. And,

$$K_{i\ s}^{ex\cdot ex} = \frac{(p.f.)_{is}^{ads}}{(p.f.)_{i}^{ads}(p.f.)_{s}^{fr}} \exp(-\Delta E_{is}/RT). \tag{14}$$

where $(p.f.)_{is}^{ads}$ is the partition function of the *ifs* triplet and ΔE_{is} is the association energy of the *i*th cation-fixed anion complex with a free *s*th cation (non-activated).

Summarizing, one may write equation 5 in the following form:

$$(V_i^{inw})_{total} = A[p_i^+]_{ex} + \frac{BK_i^{ex}[p_i^+]_{ex}}{C + K_i^{ex}[p_i^+]_{ex} + K_j^{ex}[p_j^+]_{ex}} \left(\exp\left(-\frac{\Delta F_{if}^{\ddagger}}{RT}\right) + \frac{K_{ii}^{ex\cdot ex}[p_i^+]_{ex} \exp\left(-\frac{\Delta F_{ifi}^{\ddagger}}{RT}\right) + K_{ij}^{ex\cdot ex}[p_j^+]_{ex} \exp\left(-\frac{\Delta F_{ifj}^{\ddagger}}{RT}\right)}{D + K_{ii}^{ex\cdot ex}[p_i^+]_{ex} + K_{ij}^{ex\cdot ex}[p_j^+]_{ex}}\right). \tag{15}$$

where $\Delta F_{if}^{\ddagger}$ is the free energy of activation of the *i*th ion by the doublet route and,

$$\Delta F_{if}^{\ddagger} = -RT \ln \frac{(p.f.)_{if}^{\ddagger}}{(p.f.)_{i}^{ads}} + \epsilon_{if}. \tag{16}$$

$\Delta F_{ifj}^{\ddagger}$ is the free energy of activation of the *i*th ion by the "*is*" triplet route and,

$$\Delta F_{ifj}^{\ddagger} = -RT \ln \frac{(p.f.)_{ifj}^{\ddagger}}{(p.f.)_{is}^{ads}} + \epsilon_{ifj}. \tag{17}$$

Further,

$$A = \lambda_{sal}^2 \frac{kT}{h} \cdot A_{sal} \cdot \tau_{is} \frac{(p.f.)_{i}^{\ddagger}}{(p.f.)_{i}^{fr}} \exp(-\epsilon_i/RT), \tag{18}$$

and, for simplicity of calculations, we assume

$$B = \lambda_{dbt}^2 \frac{kT}{h} \{f\} \tau_{if} l_{if} \frac{(p.f.)_{if}^{\ddagger}}{(p.f.)_{i}^{ads}} = \lambda_{tpt}^2 \frac{kT}{h} \{f\} \tau_{ifs} l_{ifs} \frac{(p.f.)_{ifs}^{\ddagger}}{(p.f.)_{is}^{ads}}. \tag{19}$$

In reference to equation 5,

$$V_i^{max} = \lambda_{dbt}^2 \frac{kT}{h} \tau_{if} l_{if} \{f^-\} \frac{(p.f.)_{if}^{\ddagger}}{(p.f.)_{i}^{ads}} \exp(-\epsilon_{if}/RT), \tag{20}$$

$$V_{ii}^{max} = \lambda_{tpt}^2 \tau_{ifi} l_{ifi} \{f^-\} \frac{(p.f.)_{ifi}^{\ddagger}}{(p.f.)_{i}^{ads}} \exp(-\epsilon_{ifi}/RT), \tag{21}$$

and

$$V_{ij}^{max} = \lambda_{tpt}^2 \frac{kT}{h} \tau_{ifj} l_{ifj} \{f^-\} \frac{(p.f.)_{ifj}^{\ddagger}}{(p.f.)_{ij}^{ads}} \exp(-\epsilon_{ifj}/RT). \tag{22}$$

In calculating the theoretical curves shown in Figs. 2, 3, 4, and 5 according to equation 15, a number of parameters were varied to demonstrate the various types of action one external ion may exercise on the rate of entry of another. These parameters fall into several categories: (*a*) universal physical constants such as the Boltzmann constant, *k*, the Planck constant, *h*, gas constant, *R*, etc. present no problem; (*b*) absolute temperature, *T*, ionic concentration $[p_i^+]_{ex}$, $[p_s^+]$, etc. which are parameters chosen for the experiments also present no problem; (*c*) free energies of activation are chosen on the basis of experimental data

(reference 6, chapter 11; 28); so are the association constants (see reference 18); (*d*) the concentration of fixed ionic sites was estimated on the basis of the maximum number of adsorption sites in the entire muscle cell (250 mmole/kg) (18), the known surface/volume ratio of frog sartorius muscle (550 cm^2/gm) (reference 6, Table 8.7) and the assumption that the density of surface ionic sites per cm^2 is the same as the average density throughout the protoplasm (*e.g.*, 4.0×10^{-8} mole/cm^2). Since we assumed that an "activated complex" is formed in the saltatory migration (see reference 6, chapter 11), the A_{sal} of equation 6 is given in moles of sites per cm^2; this is the same as the fixed anionic sites on the cell surface. (*e*) Values of the distance between two successive positions in diffusion, λ, (10^{-8} to 10^{-7} cm); the transmission coefficient (1), the libration factor (10^{-1} to 10^{-2}); the partition function ratios for the activated state [*e.g.*, $(p.f.)_{i,f}^{\ddagger}$ $(p.f.)_i^{sds}$ (10^{-1} to 1)] are reasonable figures compatible with analogous parameters determined in other diffusion studies (34, 40).

Thus, although it is not our purpose in this paper to emphasize the *quantitative* behavior of the present theoretical model, it should be pointed out that the predicted rates of permeation are of the correct order of magnitude.

This investigation was supported in part by the National Institutes of Health Research Grant GM-11422-01, and by a research grant from the National Science Foundation (GB-13). The investigator was also supported by a Public Health Service Research Development Fund GM K 3-19032.

We thank Dr. Frank Elliott, Dr. George Karreman, and Dr. Margaret Neville for their critical reading of the manuscript, and Dr. L. Kushnir for his technical assistance.

Received for publication, February 11, 1965.

REFERENCES

1. OVERTON, E., *Viertel jahrsschr. naturforsch. Ges. Zurich,* 1895, **40,** 159; and OVERTON, E., *Jahrb. wissensch. Bot.,* 1900, **34,** 669.
2. OSTERHOUT, W. J. V., *Bacterial. Rev.,* 1936, **2,** 283; and OSTERHOUT, W. J. V., *Cold Spring Harbor Symp. Quant. Biol.,* 1940, **8,** 51.
3. JACQUES, M., *J. Gen. Physiol.,* 1936, **19,** 397.
4. EPSTEIN, E., and HAGEN, C. E., *Plant Physiol.,* 1952, **27,** 457; and NEVILLE, M. C., The action of calcium ion on the entry of the monovalent cations into barley roots, Ph.D. thesis, University of Pennsylvania, 1962.
5. LING, G. N., *Proc. 19th Internat. Physiol. Cong.,* Montreal, 1953, 566; LING, G. N., *Am. J. Phys. Med.,* 1955, **34,** 89; and LING, G. N., *J. Gen. Physiol.,* 1960, **43,** suppl. 149.
6. LING, G. N., A Physical Theory of the Living State: The Association-Induction Hypothesis, New York, Blaisdell Publishing Co., 1962.
7. CONWAY, E. J., and DUGGAN, F., *Biochem. J.,* 1958, **68,** 265.
8. DANIELLI, J. F., *in* Recent Development in Cell Physiology, (J. A. Kitching, editor), London, Butterworth & Co., Ltd., 1954, 1.
9. MICHAELIS, L. M., *Bull. Nat. Research Council,* 1929, **69,** 1.
10. TEORELL, T., *Progr. Biophysics and Biophysic. Chem.,* 1953, **3,** 305.
11. SOLLNER, K., *J. Phys. and Colloid. Chem.,* 1949, **53,** 1211.
12. LING, G. N., *Am. J. Physiol.,* 1951, **167,** 806.
13. LING, G. N., *Symp. Phosphorus Metabolism,* (W. D. McElroy and B. Glass, editors), Baltimore, Johns Hopkins Press, 1952, **2,** 748.
14. LING, G. N., *Ann. New York Acad. Sc.,* 1965, **125,** 401.
15. LING, G. N., *Fed. Proc. Symp.,* 1965, **24,** S-103.
16. WILBRANDT, W., and ROSENBERG, T., *Pharm. Rev.,* 1961, **13,** 109.
17. SEN, A. K., and WIDDAS, W. F., *J. Physiol.,* 1962, **160,** 392, 404.
18. LING, G. N., and OCHSENFELD, M. M., *J. Gen. Physiol.,* in press.

19. COLOWICK, S. P., and KAPLAN, N. O., editors, Methods in Enzymology, New York, Academic Press, Inc., 1955 through 1957.
20. MULLINS, L. J., *J. Cell. and Comp. Physiol.*, 1939, **14**, 403.
21. BROOKS, S. C., *J. Cell. and Comp. Physiol.*, 1940, **16**, 383.
22. SHEPPARD, C. W. and BEYL, G. E., *J. Gen. Physiol.*, 1951, **34**, 691.
23. FRIEDMAN, A. M., and KENNEDY, J. W., *J. Am. Chem. Soc.*, 1955, **77**, 4499.
24. ALEXANDER, P., and HUDSON, R. F., Wool, Its Chemistry and Physics, New York, Reinhold Publishing Corp., 1954.
25. STEINHARDT, J., and HARRIS, M., *J. Research Nat. Bur. Std.*, 1940, **24**, 335.
26. LING, G. N., and GERARD, R. W., *J. Cell. and Comp. Physiol.*, 1949, **34**, 383.
27. HARVEY, E., and COLLANDER, R., *J. Franklin Inst.*, 1932, **1**, 214.
28. HARVEY, E., and SHAPIRO, H., *J. Cell. and Comp. Physiol.*, 1954, **5**, 255.
29. COLE, K. S., *J. Cell. and Comp. Physiol.*, 1932, **1**, 1.
30. ROBERTSON, J. D., *Biochem. Soc. Symp.*, 1959, **16**, 3.
31. BREGMAN, J. I., *Ann. New York Acad. Sc.*, 1937, **57**, 125.
32. TANDFORD, *Advances Protein. Chem.*, 1962, **17**, 69.
33. PFEFFER, W., Osmotische Untersuchungen, 2nd edition, Leipzig, W. Engelman, 1921.
34. GLASSTONE, S., LAIDLER, K. J., and EYRING, H., The Theory of Rate Processess, New York, McGraw-Hill Book Company, 1941.
35. PELZER, H., and WIGNER, E., *Z. physik. Chem.*, 1932, **B15**, 445.
36. EVANS, M. G., and POLANYI, M., *Trans. Faraday Soc.*, 1935, **31**, 875.
37. EYRING, H., *Chem. Rev.*, 1935, **17**, 65.
38. STEARN, A. E., and EYRING, H., *J. Phys. Chem.*, 1940, **44**, 955.
39. BARRER, R. M., *Trans. Faraday Soc.*, 1942, **78**, 78.
40. JOST, W., Diffusion in Solids, Liquids and Gases, New York, Academic Press, Inc., 1960.